Molecular Biology of the Cell
Vol. 15, 58–70, January 2004

Modification of a Ubiquitin-like Protein Paz2 Conducted Micropexophagy through Formation of a Novel Membrane Structure

Hiroyuki Mukaiyama,* Misuzu Baba,†‡ Masako Osumi,† Satoshi Aoyagi,* Nobuo Kato,* Yoshinori Ohsumi,‡ and Yasuyoshi Sakai*‡§

*Division of Applied Life Sciences, Graduate School of Agriculture, Kyoto University, Kitashirakawa-Oiwake, Sakyo-ku, Kyoto 606-8502, Japan; †Department of Chemical and Biological Sciences, Faculty of Science, Japan Women's University, Mejirodai, Bunkyo-ku, Tokyo 112-8681, Japan; and ‡Department of Cell Biology, National Institute for Basic Biology, Okazaki, 444-8585, Japan

Submitted May 28, 2003; Revised August 17, 2003; Accepted August 22, 2003
Monitoring Editor: Randy Schekman

Microautophagy is a versatile process in which vacuolar or lysosomal membranes directly sequester cytosolic targets for degradation. Recent genetic evidence suggested that microautophagy uses molecular machineries essential for macroautophagy, but the details of this process are still unknown. In this study, a ubiquitin-like protein Paz2 essential for micropexophagy in the yeast *Pichia pastoris* has been shown to receive modification through the function of Paz8 and Gsa7, yielding a modified form Paz2-I, similar to the ubiquitin-like lipidation of Aut7 that is essential for macroautophagy in *Saccharomyces cerevisiae*. We identified a novel membrane structure formed after the onset of micropexophagy, which we suggest is necessary for the sequestration of peroxisomes by the vacuole. Assembly of this newly formed membrane structure, which is followed by localization of Paz2 to it, was found to require a properly functioning Paz2-modification system. We herein show that Paz2 and its modification system conduct micropexophagy through formation of the membrane structure, which explains the convergence between micropexophagy and macroautophagy with regard to de novo membrane formation.

INTRODUCTION

Autophagy is a cellular process in which proteins and organelles are delivered to and degraded in lysosomes or vacuoles. Two modes of autophagy exist: microautophagy and macroautophagy. Microautophagy is the sequestration of targeted cytosolic components (including organelles) by enclosure in lysosomal or vacuolar membranes; during this process, lysosomes/vacuoles form invaginations or protrusions by generating new compartments (Klionsky and Ohsumi, 1999; Mukaiyama *et al*., 2002). This ubiquitous process is observed in cells ranging from yeast (Tuttle and Dunn, 1995; Muller *et al*., 2000) to higher mammalian and plant cells (Mortimore *et al*., 1983, 1988; Toyooka *et al*., 2001). Macroautophagy refers to the sequestration of cytosol and organelles by membranes to generate autophagosomes that then fuse with lysosomes or vacuoles, releasing autophagic bodies that are degraded within (Klionsky and Ohsumi, 1999). In both yeast and mammalian cells, macroautophagy-mediated bulk protein degradation is induced by certain nutritional states such as nitrogen starvation. Microautophagy and macroautophagy seem to differ considerably in their membrane dynamics. In macroautophagy, the newly generated isolation membrane sequesters a portion of cytoplasm first, whereas in microautophagy, vacuolar membranes engulf and sequester the target components directly and autophagosome formation does not occur.

The number of organelles (e.g., peroxisomes) per cell varies as cells adapt to surrounding stimuli. This is controlled by a combination of organellar proliferation and degradation (Subramani, 1998; Sakai and Subramani, 2000). The selective degradation of peroxisomes, called "pexophagy," is a type of autophagy (Klionsky and Ohsumi, 1999), and, as with general autophagy, there are two types of pexophagy: macropexophagy and micropexophagy (Tuttle and Dunn, 1995).

Micropexophagy in the methylotrophic yeast *Pichia pastoris* is a dynamic event. We previously followed the dynamics of micropexophagy in vivo (Sakai *et al*., 1998) by using two markers: 1) peroxisomes were labeled with a green fluorescent protein tagged with peroxisome targeting signal type 1 (GFP-PTS1) that targets to the peroxisomal matrix, and 2) vacuolar membranes were labeled with a fluorescent dye *N*-(3-triethylammoniumpropyl)-4-(*p*-diethylaminophenylhexatrienyl) pyridinium dibromide (FM4-64). Morphological and genetic analyses suggested that micropexophagy proceeds through several stages, with different genes acting in each stage (stage 0 to stage 3) (cf. Figure 9). First, a single spherical vacuole in methanol-grown cells (stage 0) invaginates slightly (stage 1a).

Article published online ahead of print. Mol. Biol. Cell 10.1091/mbc.E03–05–0340. Article and publication date are available at www.molbiolcell.org/cgi/doi/10.1091/mbc.E03–05–0340.

§ Corresponding author. E-mail address: ysakai@kais.kyoto-u.ac.jp.

Abbreviations used: FM4-64, *N*-(3-triethylammoniumpropyl)-4-(*p*-diethylaminophenylhexatrienyl) pyridinium dibromide; GFP, green fluorescent protein (S65T mutant version); GFP-PTS1, green fluorescent protein fused to PTS1; HA, hemagglutinin-antigen; immuno-EM, immunoelectron microscope; PE, phosphatidylethanolamine; PTS1, peroxisome targeting signal type 1.

Table 1. Overlap between the micropexophagy genes in *Picha pastoris* and the macroautophagy genes in *Saccharomyces cerevisiae*

Pichia	*Saccharomyces*	Unified name[a]	Reference
Necessary for macroautohagy			
PAZ1/GSA10	*APG1*	*ATG1*	(Stromhaug *et al.*, 2001; Mukaiyama *et al.*, 2002)
PAZ2	*AUT7/APG8*	*ATG8*	(Mukaiyama *et al.*, 2002)
PAZ3	*APG16*	*ATG16*	(Mukaiyama *et al.*, 2002)
PAZ8	*AUT2/APG4*	*ATG4*	(Mukaiyama *et al.*, 2002)
PAZ9/GSA14	*APG9*	*ATG9*	(Stromhaug *et al.*, 2001; Mukaiyama *et al.*, 2002)
GSA7/PAZ12	*APG7/CVT2*	*ATG7*	(Yuan *et al.*, 1999; Mukaiyama *et al.*, 2002)
GSA11/PAZ7	*APG2*	*ATG2*	(Stromhaug *et al.*, 2001; Mukaiyama *et al.*, 2002)
GSA12	*AUT10/CVT18*	*ATG18*	(Stromhaug *et al.*, 2001)
GSA20	*AUT1/APG3*	*ATG3*	(Stromhaug *et al.*, 2001)
Necessary for the CVT pathway but not for macroautophagy			
GSA9/PAZ6	*CVT9*	*ATG11*	(Kim *et al.*, 2001; Mukaiyama *et al.*, 2002)
Necessary for pexophagy but not for macroautophagy or Cvt pathway			
PAZ4	*UGT51*	*ATG26*	(Oku *et al.*, 2003)

[a] Recently, autophagy-related genes from several yeast species have been unified as *ATG* genes. See "Note added in proof" for unified nomenclature of genes.

Then, vacuoles form a new vacuolar compartment next to the peroxisomal cluster (stage 1b). This event is repeated until the peroxisomal cluster is almost completely surrounded by multiple vacuolar compartments (stage 1c). Vacuolar engulfment of peroxisomes is completed upon the sequestration of the cargo by opposing vacuolar membranes, possibly by homotypic fusion, forming a micropexophagic body (stage 2). At stage 3, soluble peroxisomal marker GFP-PTS1 diffuses into the lumenal space of the vacuole, indicating compromise of the peroxisomal membranes (Sakai *et al*., 1998; Mukaiyama *et al*., 2002). Recently, nearly 20 *PAZ/GSA* genes essential for micropexophagy were identified by high-throughput gene-tagging mutagenesis (Stromhaug *et al*., 2001; Mukaiyama *et al*., 2002). Among these, at least nine *PAZ/GSA* genes were shown to overlap with *APG/AUT* genes required for macroautophagy (Table 1) (Stromhaug *et al*., 2001; Mukaiyama *et al*., 2002). This was unexpected because the direct vacuolar engulfment of target components such as peroxisomes during microautophagy does not require the formation of cargo-containing vesicles, that is, autophagosomes.

Paz2, a *Pichia* homolog of *Saccharomyces cerevisiae* Aut7/Apg8, is a ubiquitin-like protein (Mukaiyama *et al*., 2002). Unlike other ubiquitin-like proteins, Aut7 accepts lipid modification after processing by Aut2/Apg4 through a conjugation system sequentially catalyzed by Apg7 (E1) and Aut1/Apg3 (E2) (Ichimura *et al*., 2000; Ohsumi, 2001). The *Pichia* homologs of Aut2, Apg7, and Aut1, are Paz8, Gsa7/Paz12, and Gsa20, respectively (Table 1) (Stromhaug *et al*., 2001; Mukaiyama *et al*., 2002). Furthermore, Aut7 is localized to the isolation membrane and autophagosome during macroautophagy, and as such, autophagosome formation has been traced using an Aut7 marker (Kirisako *et al*., 1999; Huang *et al*., 2000).

In this study, we examined Paz2 and its modifications before and during micropexophagy together with the intracellular dynamics of Paz2. Paz2 suppressed vacuolar engulfment of peroxisomes before the onset of micropexophagy. This process did not require modification of Paz2. We identified a novel membrane structure observed during micropexophagy that attached to the peroxisomal surface. The Paz2-modification system was necessary for localization of Paz2 to this membrane structure and perhaps for its formation. These results suggest that the identified membrane structure is a crucial structure for sequestration of peroxisomes from the cytosol for completion of micropexophagy.

MATERIALS AND METHODS

P. pastoris Strains and Plasmid Construction

The original host strain used in this work was *P. pastoris* strain PPY12 (*arg4, his4*). DNA fragments containing pREMI-Z recovered from the original *paz* mutant cells were introduced into each *PAZ* gene of strain PPY12 via homologous recombination. The resultant *paz* mutant strains (strain PPM408, PPM412, PPM401) were used in further analyses. All of the *Pichia* strains used are listed in Table 2.

The *P. pastoris-Escherichia coli* shuttle vectors pSG560 (Gould *et al*., 1992) and pHM100 were used as backbone plasmids to introduce various DNA fragments into *P. pastoris*. pHM100 was generated by inserting the polymerase chain reaction-amplified *HIS4* gene into the *Nae* I site of pBluescript II SK+. Construction of the hemagglutinin antigen (HA)-Paz2–expressing plasmids pHM104 (HA-Paz2), pHM106 (HA-Paz2 G116), and pHM107 (HA-Paz2 G116A) were described previously (Mukaiyama *et al*., 2002). pHM108 (GFP-Paz2), pHM109 (GFP-Paz2 G116), and pHM110 (GFP-Paz2 G116A) were constructed from pHM105, pHM106, and pHM107, respectively, through replacement of the 0.2-kb *Pst*I fragment of the HA tag with the 0.7-kb *Pst*I fragment harboring green fluorescent protein (GFP) S65T (BD Biosciences Clontech, Palo Alto, CA). These constructed plasmids were linearized with *Stu*I before transformation.

A DNA fragment containing the *ARG4* gene and *E. coli ori* regions was amplified using primers 5′-TGAGCTCGCGGCCGCCCTATAGTGAGTCGT-3′ and 5′-TGGATCCTGCAGGTTACAATAGTGTGTATT-3′ with pSG560 as a template, and the amplified fragment was self-ligated, yielding pHM111. The zeocin resistance gene on the *PAZ2* disruption vector was replaced with the *ARG4* fragment, which was polymerase chain reaction-amplified with the primers 5′-GGGGTACCTGCAGGAACGAAAACTCACGTTAAGGGATT-3′ and 5′-ATGAGCTCGCGGCCGCGAGTAGAAACATTTTGAAGCTATGGTG-3′, by using pHM101 as a template. This amplified fragment was *Not*I-*Pst*I digested and ligated into a *Not*I-*Pst*I-digested pHM111 vector, yielding the *PAZ2*-disruption vector with the *ARG4* gene, pHM112. pHM112 was linearized with *Eco*RI before *PAZ2* gene disruption by using the *ARG4* marker in *Pichia* cells. Proper gene disruption was confirmed by Southen blot analysis as described previously (Sakai *et al*., 1991).

Morphological Analysis

P. pastoris cells were initially grown at 28°C on a semisynthetic medium (yeast nitrogen base/methanol; YNM) containing 0.67% yeast nitrogen base without amino acids (Difco, Detroit, MI), 0.5% (vol/vol) methanol and 0.05% yeast extract, supplemented with appropriate amino acids (100 μg/ml for arginine, 100 μg/ml for histidine), and then were transferred to a rich medium (yeast extract/peptone/dextrose; YPD) containing 2% glucose, 2% bactopeptone, and 1% yeast extract to induce micropexophagy. Vacuolar membranes of methanol-grown cells were stained with FM4-64

Table 2. *P. pastoris* strains used in this study

Strain	Genotype or description	Background	Reference
PPY12	*arg4 his4*	Wt	Sakai *et al.* (1998)
PPM5010	*arg4 his 4* Δ*paz2*::pHM101 (*Zeo*)	Δ*paz2*	Mukaiyama *et al.* (2002)
PPM5011	PPM5010 *his4*::pHM104 (P_{PAZ2}HA-PAZ2 HIS4)	Δ*paz2*	Mukaiyama *et al.* (2002)
PPM5014	PPM5010 *his4*::pHM107 (P_{PAZ2}HA-PAZ2G116A HIS4)	Δ*paz2*	Mukaiyama *et al.* (2002)
PPM5015	PPM5010 *his4*::pHM108 (P_{PAZ2}GFP-PAZ2 HIS4)	Δ*paz2*	This study
SA1017	PPY12 *arg4*::pSAP115 (P_{PAZ2}YFP-PAZ2 ARG4)	Δ*paz2*	This study
PPM5016	PPM5010 *his4*::pHM106 (P_{PAZ2}HA-PAZ2G116 HIS4)	Δ*paz2*	Mukaiyama *et al.* (2002)
PPM5017	PPM5010 *his4*::pHM110 (P_{PAZ2}GFP-PAZ2G116A HIS4)	Δ*paz2*	This study
PPM408	*arg4 his4 paz8*::pREMI-Z (*Zeo*)	*paz8*	Mukaiyama *et al.* (2002)
PPM5030	*arg4 his4 paz8*::pREMI-Z (*Zeo*) Δ*paz2*::pPM112 (*ARG4*)	Δ*paz2 paz8*	This study
PPM5032	PPM5030 *his4*::pHM106 (P_{PAZ2}HA-PAZ2G116 HIS4)	Δ*paz2 paz8*	This study
PPM5033	PPM5030 *his4*::pHM109 (P_{PAZ2}GFP-PAZ2G116 HIS4)	Δ*paz2 paz8*	This study
PPM412	*arg4 his4 paz12*::pREMI-Z (*Zeo*)	*paz12*	Mukaiyama *et al.* (2002)
PPM5040	PPM412 Δ*paz2*::pHM112 (*ARG4*)	Δ*paz2 gsa7*	This study
PPM5041	PPM5040 *his4*::pHM104 (P_{PAZ2}HA-PAZ2 HIS4)	Δ*paz2 gsa7*	This study
PPM5042	PPM5040 *his4*::pHM108 (P_{PAZ2}GFP-PAZ2 HIS4)	Δ*paz2 gsa7*	This study
PPM401	*arg4 his4 paz1*::pREMI-Z (*Zeo*)	*paz1*	Mukaiyama *et al.* (2002)
PPM5050	PPM401 Δ*paz2*::pHM112 (*ARG4*)	Δ*paz2 paz1*	This study
PPM5052	PPM5050 *his4*::pHM108 (P_{PAZ2}GFP-PAZ2 HIS4)	Δ*paz2 paz1*	This study

in 5 ml of YNM medium as described previously (Sakai *et al*., 1998). For *paz* mutant analysis, YNM-grown cells were collected by centrifugation, further cultured at 28°C in 5 ml of YPD medium and were examined at appropriate time intervals by fluorescence microscopy.

Fluorescently labeled cells were examined under an IX70 fluorescence microscope (Olympus, Tokyo, Japan) by using a XF52 filter set (Omega Optical, Brattleboro, VT) for FM4-64 and fluorescent proteins. Image data were captured with a SenSys charged-coupled device camera (PhotoMetrics, Huntington Beach, CA) by using MetaMorph version 4.6 (Universal Imaging, Downingtown, PA) and were saved as Adobe Photoshop files (Adobe Systems, Tokyo, Japan) on a Epson Endeavor MT-4500 computer.

Biochemical Methods

Anti-HA monoclonal antibody was purchased from F. Hoffmann-La Roche (Basel, Switzerland). Anti-GFP antiserum was kindly provided by Dr. M. Fransen (Katholieke Universiteit, Louvain, Belgium).

Standard 12.5% Laemmli gels (SDS-PAGE) or SDS gels containing 6 M urea (Urea-SDS-PAGE), with the separating gel at pH 9.2, were used. Cell lysates containing 10 μg of protein prepared from the cells were loaded on each lane. The gels were transferred to nitrocellulose transfer membranes (Schleicher & Schuell, Keene, NH) at 14 V overnight in a cold room and were blocked using 5% skim milk in Tris-buffered saline-Tween 20 (TBS-T) buffer (containing 2.42 g of Tris base, 8 g of NaCl/l, pH 7.6). Blots were rinsed three times for 10 min each in TBS-T and incubated with anti-HA mAb (1:2000 dilution) in TBS-T for 60 min under gentle shaking. Blots were rinsed three times in TBS-T, incubated with peroxidase-conjugated anti-rabbit antibody or with peroxidase-conjugated anti-mouse antibody. Blots were rinsed in TBS-T and detected with an enhanced chemiluminescence detection kit (Amersham Biosciences, Piscataway, NJ).

Subcellular Fractionation

Subcellular fractionation experiments were performed as described previously (Horazdovsky and Emr, 1993). Cells were cultured in YNM medium at 28°C to OD_{610} = 1.0–1.2 (1–2 × 10^7 cells/ml), collected, and transferred to YPD medium for 1 h to induce micropexophagy. Harvested cells were converted to spheroplasts in each of the following spheroplasting media: 1) cells before micropexophagy: 0.67% yeast nitrogen base without amino acids and ammonium sulfate, 1.2 M sorbitol, 20 mM Tris-HCl, pH 7.5, 0.5% methanol, and 37.5 $\mu g/10^8$ cells of zymolyase 100T (Seikagaku Kogyo, Japan); and 2) cells undergoing micropexophagy: 1% yeast extract, 2% peptone, 2% glucose, 1.2 M sorbitol, 20 mM Tris-HCl, pH 7.5, and 25 $\mu g/10^8$ cells of zymolyase 100T. Spheroplasts were harvested and rinsed with a lysis buffer containing 0.2 M sorbitol, 50 mM Tris-HCl, pH 7.5, 1 mM ethylenediamine-*N*,*N*,*N*′,*N*′-tetraacetate, 1 mM phenylmethylsulfonyl fluoride, and a protease inhibitor cocktail; F. Hoffmann-La Roche). Total lysates (T) were generated by centrifugation at 500 × *g* for 3 × 5 min and then spun at 13,000 × *g* for 15 min to separate into pellet (LSP) and supernatant (LSS) fractions. The LSS fraction was then centrifuged at 100,000 × *g* for 1 h on a Beckman Coulter Optima TLX 100 ultracentrifuge, yielding a pellet fraction (HSP) and a supernatant fraction (HSS). LSP and HSP fractions were resuspended in equal volumes of the lysis buffer to the original lysates. Equal volumes of each sample were subjected to SDS-PAGE or urea-SDS-PAGE.

Electron Microscopy

Preparation of *Pichia* cells for electron microscopy was done according to procedures described previously (Baba *et al*., 1997) with slight modifications. In brief, cells were transferred to 2% osmium tetroxide and 0.5% glutaraldehyde in cold absolute acetone. Substitution fixation was carried out at −80°C for 2 d, and then at −25°C overnight. Samples for immunoelectron microscopy (EM) analysis were prepared as described previously (George *et al*., 2000). GFP was immunolabeled with anti-GFP polyclonal antibody (1:300 dilution) for 2 h at room temperature. The sections were stained with 4% uranyl acetate for 10 min and with 0.2% lead citrate for 1 min. Ultrathin sections were examined with an electron microscope (model H-800; Hitachi, Tokyo, Japan) at 125 kV.

RESULTS

Paz2-Modification in P. pastoris

Many of *Pichia* strains isolated as micropexophagy-deficient mutant strains (including *paz2*, *paz8*, *gsa7/paz12*, and *gsa20* strains) turned out to be impaired in *APG*-homolog genes (Table 1) (Stromhaug *et al*., 2001; Mukaiyama *et al*., 2002). In this study, we examined the role of the Paz2-modification system in micropexophagy.

In *S. cerevisiae*, the Gly116 residue at the carboxy terminus of Aut7 is exposed through processing by the cystein protease Aut2 and then is lipidated by a ubiquitination-like system (Ichimura *et al*., 2000; Kirisako *et al*., 2000). A G116A mutation in Aut7 abolishes Aut7 lipidation. To follow Paz2 modification in *P. pastoris*, an HA-Paz2 fusion protein and two mutated forms, HA-Paz2 with a Gly116 residue as a carboxy terminus (HA-Paz2 G116) and HA-Paz2 with a Gly116Ala mutation (HA-Paz2 G116A), were expressed in the *paz2*Δ strain. The Paz2 proteins were separated by SDS-PAGE and subjected to immunoblot analysis by using an anti-HA antibody (Figure 1A).

Cell lysates from both the HA-Paz2- and HA-Paz2 G116-expressing cells gave a single 20-kDa band (Figure 1A, top, lanes 1 and 2), whereas cell lysate from the HA-Paz2 G116A-expressing cells gave a single 21-kDa band (Figure 1A, lane 3). The band size difference of 1 kDa is consistent with the molecular weight of a nine-residue amino acid cleaved from the carboxy terminus upon pro-

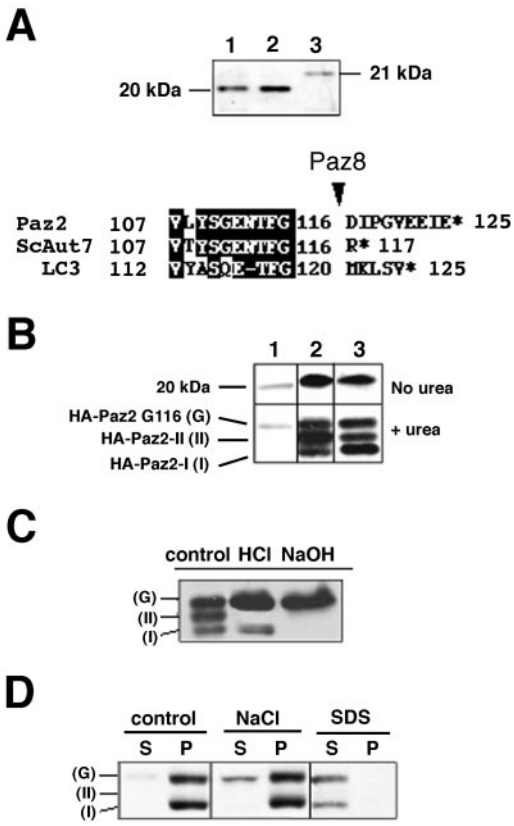

Figure 1. Processing of HA-Paz2 by Paz8 and the following modification of HA-Paz2 in *P. pastoris*. (A) Top, processing of HA-Paz2 by Paz8 is inhibited by the G116A mutation on Paz2. Immunoblot analysis of HA-Paz2 proteins after standard SDS-PAGE. The following proteins were expressed in the *paz2*Δ background: lane 1, HA-Paz2 (strain PPM5011); lane 2, HA-Paz2 G116 (strain PPM5016); lane 3, HA-Paz2 G116A (strain PPM5014). Bottom, amino acid sequence alignment of the carboxyl terminal region of Paz2 and its homologs, *S. cerevisiae* Aut7 and mouse LC3. Paz8 is thought to be hydrolyzed at the carboxyl moiety of the Gly 116 residue on Paz2, releasing a nine-amino acid peptide. (B–D) Modified forms of HA-Paz2 detected on SDS-PAGE containing 6 M urea followed by immunoblot analysis. The mobilities of HA-Paz2-I (I), HA-Paz2-II (II), and HA-Paz2 G116 (G) on urea-SDS-PAGE are indicated at left from bottom to top. (B) HA-Paz2 cells (strain PPM5011) were pregrown on glucose-medium (lane 1) and transferred to methanol-containing medium to induce peroxisomes for 12 h (lane 2). Then, the cells were transferred to glucose-containing medium to induce micropexophagy for 1 h (lane 3). At each time point, cell lysates were prepared, and the same amount of protein (10 μg) was subjected to SDS-PAGE (bottom) with or (top) without 6 M urea, followed by immunoblot analysis. (C) Before loading, the sample from Figure 1B, lane 3, was supplemented with HCl or NaOH to a final concentration of 0.2 M, incubated on ice for 1 h, and then dialyzed against a lysis buffer. (D) HA-Paz2-I behaves like an integral membrane protein. Cell lysates from HA-Paz2 cells (strain PPM5011) were sonicated and spun at 100,000 $\times$ *g* for 1 h to generate a pellet. The pellets were suspended in lysis buffer (without sorbitol) containing 1% SDS, or 1 M NaCl, chilled on ice for 30 min, and centrifuged again at 100,000 $\times$ *g* for 1 h to separate the supernatant and pellet. The pellet was resuspended in an amount of lysis buffer equal to that of the original sample. Proteins recovered in each fraction were precipitated with 10% trichloroacetic acid and resuspended in the SDS sample buffer. Equal volumes of each sample were subjected to urea-SDS-PAGE and detected by immunoblot analysis.

teolytic processing (Figure 1, bottom). Therefore, as with Aut7, the G116A mutation in Paz2 caused loss of HA-Paz2-processing. When HA-Paz2 was expressed in the *paz8* mutant, HA-Paz2 was not processed, giving rise to a 21-kDa band upon SDS-PAGE of the cell lysate (our unpublished data). These results demonstrate that processing of Paz2 is very similar to that of Aut7, that is, Paz2 is processed by Paz8 and the processing is inhibited by the G116A mutation.

Next, cell lysate of HA-Paz2–expressing cells was subjected to SDS-PAGE containing 6 M urea (urea-SDS-PAGE) under the same conditions used to separate modified forms of Aut7 (Ichimura *et al*., 2000). The sample from the HA-Paz2 cells showed three bands of different mobilities (top, middle, and bottom bands; Figure 1B, lanes 2 and 3). Figure 1C shows the band pattern when cell lysate containing HA-Paz2 was treated with 0.2 M NaOH or 0.2 M HCl. The top band was stable against the two treatments. The bottom band was sensitive to alkaline treatment but was resistant to acid treatment. The middle band was sensitive to both treatments. Because the middle and bottom bands shifted to the top band as a result of acid and alkaline treatments, the middle and bottom bands were considered to represent modified forms of the top band, that is, HA-Paz2 G116. The modified forms of HA-Paz2 were designated as HA-Paz2-I (bottom band) and HA-Paz2-II (middle band) (Figure 1B). Assignment of these bands was confirmed further by results from later biochemical and mutant analyses described below.

Biochemical Characterization of Paz2-modified Forms

The two modified forms of HA-Paz2 were characterized further. Cell lysates prepared from HA-Paz2 cells before and after onset of micropexophagy were fractionated by differential centrifugation into three fractions: a LSP (pellet after 13,000 $\times$ *g*), a HSP pellet (after 100,000 $\times$ *g*), and a HSS (supernatant after 100,000 $\times$ *g*). Modified forms of HA-Paz2 in each fraction were separated by urea-SDS-PAGE and detected by immunoblot analysis as described above.

The amount of HA-Paz2 and its derivatives, together with their intracellular distribution in several *paz* mutants, is summarized in Figure 2. HA-Paz2-I was found only in the pellet fraction (Figure 2A). Similar to integral membrane proteins, it was not solubilized by 1 M NaCl or 0.1 M Na_2CO_3 (our unpublished data), but was solubilized by 1% SDS (Figure 1D). A major fraction of HA-Paz2-II was present in the HSS. These biochemical features of HA-Paz2-I resembled a lipidated form of Aut7, Aut7-phosphatidylethanol amine (Aut7-PE) (Ichimura *et al*., 2000). If HA-Paz2-I is formed through an Aut7-like conjugation pathway, HA-Paz2-I formation would be expected to be inhibited in related *paz* mutants and in the HA-Paz2 G116A cells. The band pattern of the HA-Paz2 G116 cells was the same as that of the HA-Paz2 cells (our unpublished data; cf. Figure 2A). When HA-Paz2 G116A was expressed in *paz2*Δ cells, two bands were observed that showed slightly lower mobilities than those of HA-Paz2 G116 and HA-Paz2-II (Figure 2B). The distributions of the two bands were substantially the same as those of HA-Paz2 G116 and HA-Paz2-II, and the band shift reflected the nine-residue size difference between HA-Paz2 G116A and HA-Paz2 G116. This result shows that HA-Paz2 G116A is unable to undergo modification and yield a product corresponding to HA-Paz2-I.

Expression of HA-Paz2 G116 and HA-Paz2 in the *paz8* mutant gave contrasting results. HA-Paz2 G116 was suc-

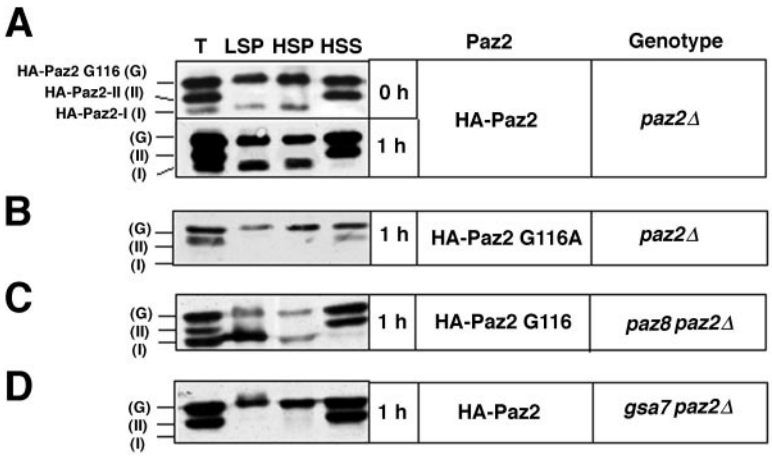

Figure 2. Subcellular fractionation of cell lysates from various *Pichia* cells expressing HA-Paz2. The expressed protein and the *Pichia* strains are as follows: (A) HA-Paz2 in *paz2*Δ cells (strain PPM5011); (B) HA-Paz2 G116A in *paz2*Δ cells (strain PPM5014); (C) HA-Paz2 G116 in *paz8 paz2*Δ cells (PPM5032); and (D) HA-Paz2 in *gsa7 paz2*Δ cells (strain PPM5041). Cells grown on methanol-containing medium (0 h) were shifted to glucose-containing medium for 1 h (1 h). At each time point, cell lysates were prepared and fractionated as described under MATERIALS AND METHODS. T, total lysates; LSP, low-speed (13,000 × *g*) pellet fraction; HSP, high-speed (100,000 × *g*) pellet fraction; HSS, high-speed (100,000 × *g*) supernatant fraction.

cessfully converted into HA-Paz2-I even in the *paz8* mutant (Figure 2C), whereas HA-Paz2 was not (our unpublished data). This indicates that HA-Paz2 was modified after exposure of the Gly116 residue. However, expression of HA-Paz2 G116 in the *paz8* mutant could not restore micropexophagy, which was arrested at stage 1c (our unpublished data). Lack of Paz8 activity, which converts HA-Paz2-I back to HA-Paz2 G116 (Kirisako *et al*., 2000), would cause accumulation of HA-Paz2-I in the cells. Indeed, the relative ratio of HA-Paz2-I to HA-Paz2 G116 was increased in HA-Paz2 G116-expressing *paz8 paz2*Δ cells (Figure 2C), compared with HA-Paz2-expressing *paz2*Δ cells (Figure 2A).

In *S. cerevisiae*, Apg7 is an E1 enzyme responsible for Aut7-lipidation as well as Apg12-conjugation (Ichimura *et al*., 2000; Kirisako *et al*., 2000). *GSA7/PAZ12*, a *Pichia APG7* homolog, was shown previously to be necessary for micropexophagy (Yuan *et al*., 1999; Mukaiyama *et al*., 2002). In *gsa7* mutant cells, HA-Paz2-I was not detected in the cell lysate of HA-Paz2–expressing cells (Figure 2D). However, the formation and intracellular distribution of HA-Paz2 G116 and HA-Paz2-II was identical to that in the wild type. These results show that, in *P. pastori*s, Gsa7 is essential for Paz2 modification, that is, the conversion of HA-Paz2 G116 to HA-Paz2-I.

From these biochemical and genetical analyses, we conclude that Paz2-I is a *Pichia* counterpart of Aut7-PE and that a corresponding Paz2 modification system is essential for pexophagy in *P. pastoris* (cf. Figure 9). The other modified form, HA-Paz2-II, was a previously unknown form of an Aut7-family protein. The notable biochemical feature of HA-Paz2-II is its exclusive localization in the soluble fraction. Its physiological function as well as its chemical structure remains to be solved.

Dynamics of GFP-Paz2 after the Onset of Micropexophagy

In glucose-grown cells, HA-Paz2 was mainly present as a form of HA-Paz2 G116 (Figure 1B, lane 1). The total amount of HA-Paz2 increased after the shift from glucose- to methanol-containing medium (Figure 1B, lane 2). The presence of a considerable amount of HA-Paz2-I might be due to induction of macroautophagy, which occurred after the shift to methanol- from glucose-containing medium. During this period (up to 6 h of methanol adaptation), GFP-Paz2 puncta representing autophagosomes were observed in the cytosol, but these GFP-Paz2 puncta disappeared after 12 h of methanol adaptation (our unpublished data). After induction of micropexophagy, the amount of pelletable HA-Paz2-I nearly doubled (Figure 1B, lanes 2 and 3; LSP and HSP fraction in Figure 2A) although the total amount of HA-Paz2 did not change (Figure 1B). These results suggest further activation of Paz2 modification at the onset of micropexophagy.

The competence of micropexophagy in the GFP-Paz2 cells was confirmed by two independent methods: alcohol oxidase degradation assay after glucose-shift and morphometric analysis of vacuolar dynamics as described previously (Sakai *et al*., 1998). Expression of GFP-Paz2 in the *paz2*Δ cells recovered alcohol oxidase-degradation competence after glucose-shift. Morphometric analysis revealed that the ratio of invaginated vacuoles (stage 1) increased after 30 min of glucose adaptation, and that the ratio of stage 2 cells increased after 1-h adaptation. The competence of micropexophagy in the GFP-Paz2 cells was confirmed by both methods to be comparable with that in wild-type cells (Sakai *et al*., 1998).

Before the induction of pexophagy, GFP-Paz2 cells showed cytosolic and vacuolar fluorescence (Figure 3A, 0 h). After 15–30 min of micropexophagy induction, one bright fluorescent structure occurred within cells. Figure 3B shows representative fluorescence images. Cells with slightly invaginated vacuoles (stage 1a) had one small punctum of GFP fluorescence at the tip of the invagination. Cells at stage 1b possessed an extended fluorescent structure between the tips of the deeply invaginating vacuole. Just before contact is made by opposing vacuolar membranes (stage 1c), GFP fluorescence was observed exclusively between them. Stage 2 cells did not exhibit bright GFP fluorescence (our unpublished data).

When the GFP-Paz2 cells were shifted to ethanol-containing medium to induce macropexophagy, a ring of GFP fluorescence, representing a pexophagosome, was observed outside the spherical vacuole (Figure 3C).

GFP-Paz2 Localizes to a Novel Membrane Structure during Micropexophagy

The GFP-Paz2 cells undergoing micropexophagy were subjected to rapid freezing and freeze-substitution fixation, and observed by electron microscopy.

Fifteen to 30 min after the onset of micropexophagy, we observed a novel membrane structure on the cytosolic surface of the clustered peroxisomes (Figure 4, A–C). This membrane structure was not observed in methanol-grown

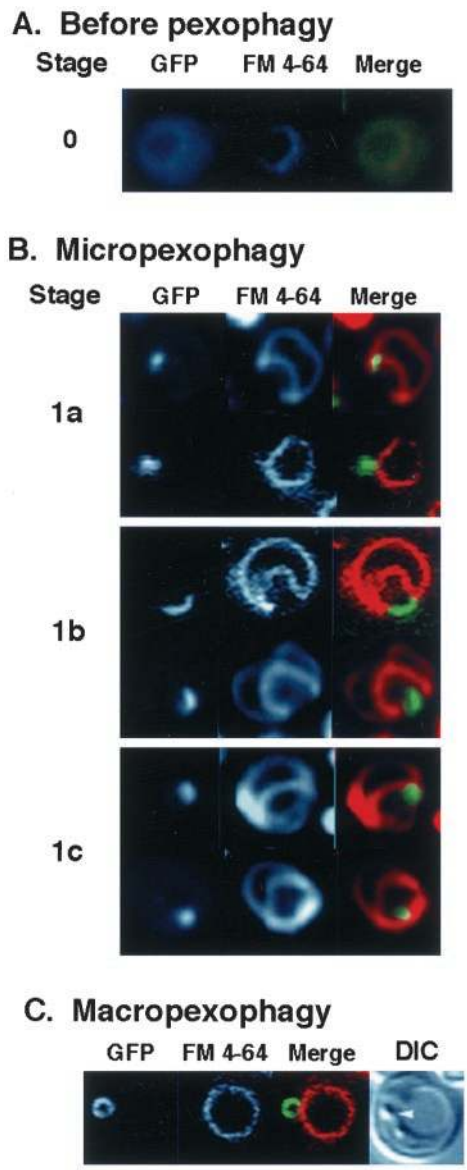

Figure 3. Dynamics of Paz2-fusion proteins before and during pexophagy. Fluorescence images of GFP-Paz2 cells (strain PPM5015) at various stages of micropexophagy. Left, GFP-Paz2 fluorescence. Middle, FM4-64. Right, merged; DIC, differential interference contrast microscopy. (A) Before micropexophagy, some GFP fluorescence was associated with vacuoles. (B) After the onset of micropexophagy for 15–30 min, GFP-Paz2 cells showed a bright fluorescent area. Representative cells from each stage of micropexophagy are shown. At early stage 1, GFP fluorescence was observed at the tip of the invaginating vacuole. At stage 1b to c, extended GFP fluorescence was observed between opposing vacuolar tips. At stage 1c, GFP-Paz2 fluorescence was observed at the point of contact of opposing vacuolar tips. (C) In contrast to the micropexophagic process, ring-shaped fluorescence was observed under macropexophagic conditions (shift to ethanol-containing medium for 15 min). Note that macropexophagy proceeded without changing the morphology of vacuoles (Sakai *et al*., 1998). An arrowhead points to a cytosolic granule that may represent the peroxisome.

cells not induced for micropexophagy (our unpublished data), and it was observed as a membrane-bound flattened sac ~20–25 nm in uniform thickness, with hardly any lumenal space and clearly distinct from both peroxisomal and vacuolar membranes (Figure 4, B and C). Immuno-EM analysis revealed that this newly formed membrane structure could be labeled specifically with gold particles coated with anti-GFP antibody, indicating localization of GFP-Paz2 (Figure 5). GFP-Paz2 localized to both cytosolic and peroxisomal sides on the membrane structure (Figure 5B).

In methanol-grown cells, peroxisomes are present in a single cluster. When the vacuole undergoes micropexophagy after the shift to glucose-containing medium, it sequesters peroxisomes as a whole cluster. In each cell, a single membrane structure attaches to one of the peroxisomes in the cluster at the far side of the invaginating vacuole (Figures 4, A and C, and 5C). Multiple numbers of such membrane structures were not seen in one cell (Figures 4A and 5C).

The Assembly of Membrane Structure Is Inhibited in Multiple paz Mutants Impaird in Paz2 Modification System

Next, the proper assembly of membrane structure was monitored by following the localization of GFP-Paz2 in *gsa7* mutant cells. In these cells, GFP-Paz2 did not show the typical bright fluorescence observed in the GFP-Paz2-complementing wild-type cells but showed mainly cytosolic fluorescence both before and after onset of micropexophagy (Figure 6A). Expression of GFP-Paz2 G116A in *paz2*Δ cells resulted in cells showing a similar cytosolic fluorescence (Figure 6A).

On the other hand, when GFP-Paz2 G116 was expressed in the *paz8* cells, micropexophagy was arrested at stage 1c (our unpublished data). We observed a bright, irregularly shaped GFP-fluorescent structure, which suggested that the proper localization of GFP-Paz2 had been inhibited (Figure 6B). These results indicate that the proper assembly of membrane structure requires the complete cycling of the Paz2 modification pathway (Paz2 G116 ↔ Paz2-I; cf. Figure 9), properly regulated by related *PAZ* gene products.

Macropexophagy and Micropexophagy Followed by Tracing YFP-Paz2 in a Single Cell

Previous studies showed that macropexophagic process could occur even after adaptation to glucose-containing medium (Tuttle and Dunn, 1995; Sakai *et al*., 1998), raising the possibility that the observed membrane structure was merely a nascent isolation membrane that did not have any function during micropexophagy. However, >70% of cells were observed to enter into micropexophagy; these cells possessed both deeply invaginated vacuoles and typical GFP-Paz2 fluorescence (Figure 3B). Furthermore, a ring of GFP-Paz2 fluorescence outside the spherical vacuole, representing the pexophagosome during macropexophagy, was scarcely observed during glucose-adaptation conditions. (Less than 2% of total cells showed such a fluorescent structure.) These results support that cells form the membrane structure to execute micropexophagy. Also, because our present results strongly suggested essentiality of the membrane structure during sequestration of peroxisomes from the cytosol, we focused on stage 1c of micropexophagy and followed the dynamics of Paz2 and vacuolar membrane (stained with FM4-64) in a single cell at this stage.

At first, we followed the macropexophagic process in ethanol-containing medium by using YFP-Paz2–expressing strain, and as shown in Figure 7A, formation of autophagosome (pos-

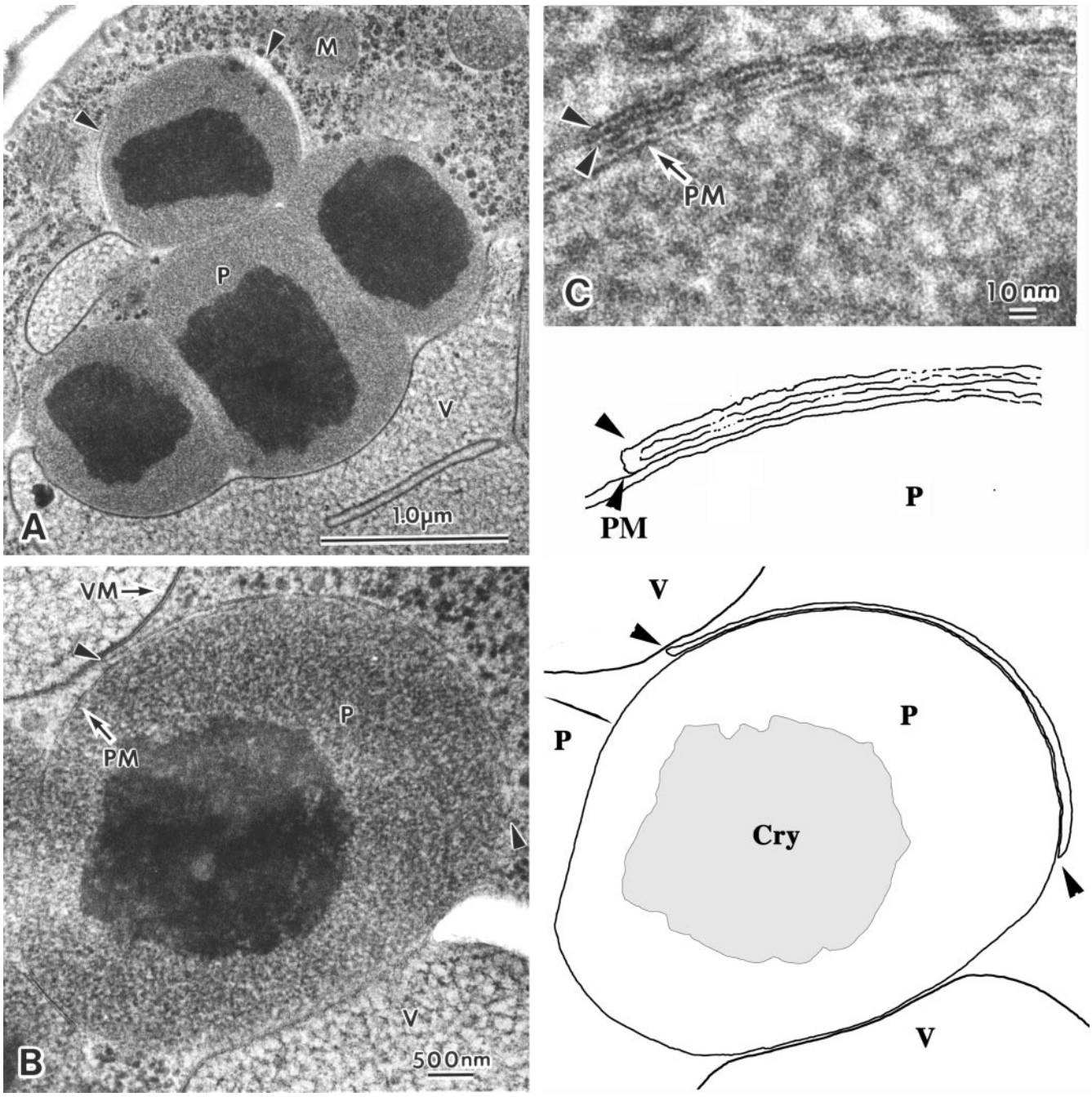

Figure 4. Morphology of the membrane structure formed during micropexophagy in GFP-Paz2 cells (strain PPM5015), which was observed under electron microscope. (A) The membrane structure was formed at the surface of the peroxisome. Arrowheads represent two ends of the membrane structure. (B) Left, the membrane structure attached to the peroxisomal surface. Right, a schematic tracing of the photograph. (C) Top, magnified image of the membrane structure and (bottom), a schematic tracing of the photograph. Because two lipid bilayers from membrane structure and one from the peroxisome could be seen at the extreme end of the membrane structure, the membrane structure is assumed to be a flattened sac attached to the peroxisomal membrane. Arrowheads indicate the membrane structure. P, peroxisome; PM, peroxisome membrane; V, vacuole; VM, vacuolar membrane; M, mitochondrion, Cry, alcohol oxidase crystalline.

sibly pexophagosome) could be followed by YFP-Paz2 fluorescence. Only after a ring-structure of YFP-Paz2 fluorescence had been formed, the formed autophagosome fused with vacuole which could be detected by staining of autophagosome membrane by FM4-64 at this time point. On fusion between vacuole and autophagosome, the intensity of YFP-Paz2 fluorescence greatly diminished or disappeared. These fluorescence images were consistent with the postulated membrane dynamics of macropexophagy (cf. Figure 9).

Next, formation of the membrane structure was followed by YFP-Paz2 fluorescence under glucose-adaptation conditions in a single cell (Figure 7B). Throughout the

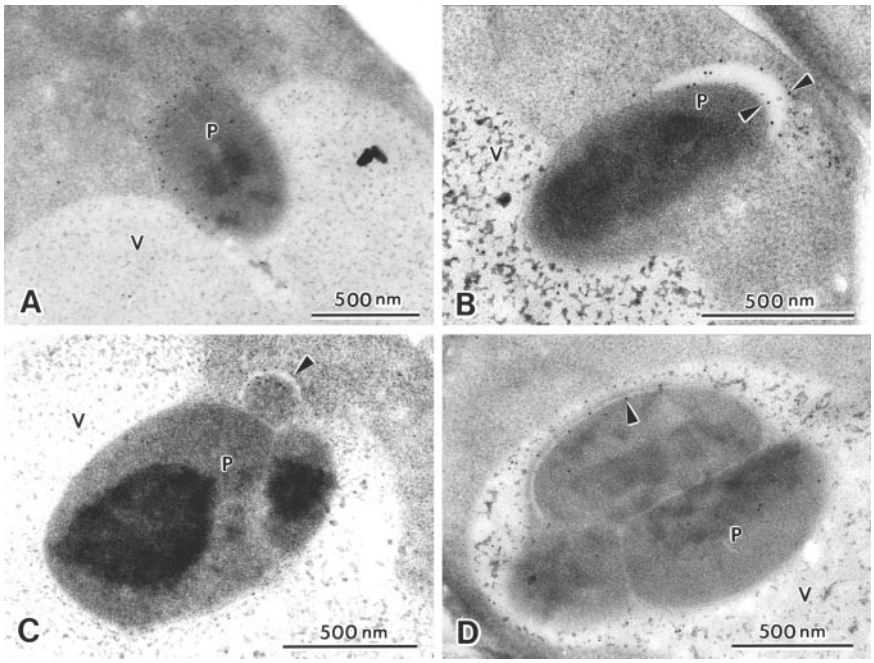

Figure 5. Immuno-EM analysis labeled with gold particles coated with anti-GFP antibody in GFP-Paz2 cells (strain PPM5015). (A–D) Localization of GFP-Paz2 to the membrane structure formed during micropexophagy. (B) The membrane structure showing a lumenal space indicates that this structure is a membrane sac. (C) In this image, a newly synthesized peroxisome, which is smaller than the others and lacks an alcohol oxidase crystalline structure, was covered with the membrane structure. (D) The membrane structure was observed to be present in the vacuole of stage 2 cell. Arrowheads indicate the membrane structure. P, peroxisomes; V, vacuoles.

micropexophagic process, YFP-Paz2 did not show a ring-like structure as observed for autophagosome, indicating that the membrane structure did not enclose a whole peroxisome. However, similar to the observation during macropexophagy, the cup-shaped YFP-Paz2 fluorescence disappeared at the time point indicated (Figure 7B, arrow heads), concomitant with an appearance of a cup-shaped FM4-64 fluorescence. This was consistent with the results obtained with GFP-Paz2 dynamics (Figure 3B), i.e., the disappearance of GFP-Paz2 fluorescence in stage 2 cells. Indeed, fluorescence images of putative stage 2 cells (Figure 7C) suggested a cup-shaped structure stained with FM4-64 attached to peroxisomes. These results suggest that the cup-shaped membrane structure fused with vacuolar membrane to sequester peroxisomes from the cytosol.

Both fluorescent and EM images of putative stage 2 cells suggested that the membrane structure was observed within the vacuole (Figures 5D and 7C). However, further experiments, i.e., serial sectioning, are necessary to demonstrate that the membrane structure is indeed incorporated into the vacuole together with a peroxisomal cluster after micropexophagy.

Vacuolar Engulfment Is Suppressed during Stage 0 in a Manner Independent of Paz2-Modification

Disruption of the *PAZ2* gene yielded aberrant vacuolar morphology in methanol-grown cells. Electron microscopy of *paz2*Δ cells showed extensive engulfment of peroxisomes and cytosol by vacuolar membranes, from which mitochondria escaped. The vacuole was observed to initiate engulfment of peroxisomes and cytosol via microautophagic process but could not complete their sequestration (Figure 8A). GFP-Paz2 G116A (corresponding to HA-Paz2 G116A that escapes Paz2-modification) restored normal vacuolar morphology in the *paz2*Δ cells (Figure 8B). As shown in Figure 8C, GFP fluorescence, associated with vacuolar membranes, was diffused throughout the cytosol, consistent with biochemical experiments identifying HA-Paz2 G116A not only in the HSP and HSS fractions but also in the vacuole-containing LSP fraction (Figure 2B). The presence of vacuoles in the LSP fraction was also monitored by FM4-64 vacuolar staining.

Although GFP-Paz2 G116A restored normal vacuolar morphology in the *paz2*Δ cells, it could not recover nitrogen starvation-induced macroautophagy and micropexophagy. Under nitrogen-starvation conditions, we observed in GFP-Paz2 G116A cells neither punctuate GFP in the cytosol, representing autophagosomes, nor GFP fluorescence in the vacuolar lumen (our unpublished data), both of which were observed in GFP-Paz2 cells. Micropexophagy in the GFP-Paz2 G116A cells was confirmed morphologically to arrest at stage 1c (our unpublished data). Many Apg-homolog *paz/gsa* mutants also demonstrated arrested micropexophagy at this stage (Mukaiyama *et al*., 2002), indicating a crucial function of Paz2 modification in completing peroxisome sequestration at stage 1c (Figure 9).

Although the *paz2*Δ cells showed defects in vacuolar morphology, overexpression of Paz2 inhibited vacuolar engulfment of peoxisomes and arrested micropexophagy at stage 1b (Mukaiyama *et al*., 2002). This genetic evidence suggests that vacuoles have an inherent tendency to engulf peroxisomes and that this tendency is suppressed during peroxisome proliferation by a negative regulatory function of Paz2. As shown in Figure 8B, GFP-Paz2 G116A restored normal vacuolar morphology in the *paz2*Δ cells. Also, *gsa7*, *paz8*, and other *APG*-homolog *paz* mutants showed normal morphology at stage 0, and the *PAZ2*-deletion phenotype with regards to vacuolar morphology at stage 0 was dominant against other *paz* mutations (Mukaiyama *et al*., 2002). These results indicate that the GFP fluorescence seen in GFP-Paz2 G116A cells reflects Paz2-mediated suppression of vacuolar engulfment of peroxisomes during stage 0, which does not require the modification of Paz2 to Paz2-I. Although HA-Paz2 G116A was found in each of the HSP, LSP, and HSS fractions, the

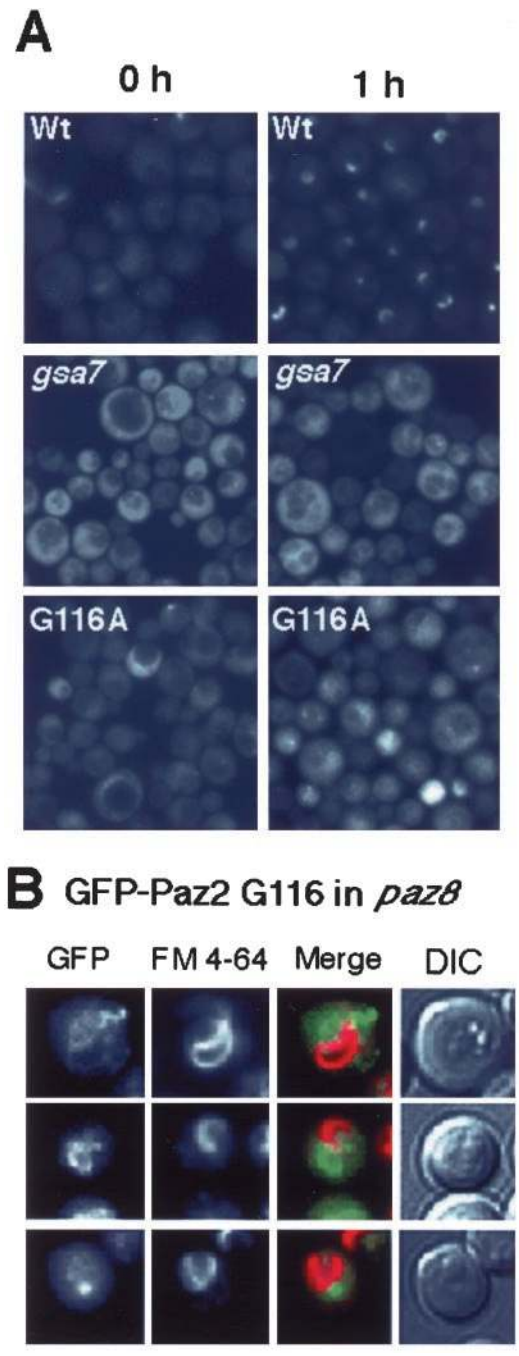

Figure 6. Assembly of the membrane structure followed by localization of GFP-Paz2 to the membrane structure is inhibited in multiple *paz* mutants. (A) GFP-Paz2–expressing cells of the wild-type strain (PPM5015), *gsa7* mutant cells (PPM5042), and GFP-Paz2 G116A cells (strain PPM5017) were grown on methanol-containing medium, and shifted to glucose-containing medium for 1 h to induce micropexophagy. (B) Fluorescence images of GFP-Paz2 G116-expressing cells in the *paz8* background (strain PPM5033). Methanol-grown cells were shifted to glucose-containing medium to induce micropexophagy for 1 h.

corresponding forms of Aut7 protein were not observed in LSP fractions in *S. cerevisiae* under the same subcellular fractionation conditions (Kirisako *et al*., 2000). This explains the association of HA-Paz2 G116A and HA-Paz2 G116 to the vacuolar membrane and their suppressive function not found in Aut7 of *S. cerevisiae*.

DISCUSSION

Multiple *PAZ/GSA* genes required for micropexophagy were identified to be Apg homologues required for macroautophagy (Table 1). Based on the sequence analysis of *PAZ* genes, Paz2 was found to be a ubiquitin-like protein, and Paz8, Gsa7, and Gsa20 seem to be involved in a putative Paz2 modification pathway. Our present biochemical and genetic evidence reveals that Paz2 in *P. pastoris* is modified to Paz2-I through a modification system similar to the Aut7-PE modification system in *S. cerevisiae*.

Through these studies on the role of Paz2-modification in micropexophagy, we found a novel membrane structure, which is formed after the onset of micropexophagy. The assembly of membrane structure, which was followed by GFP-Paz2 localization, occurred in a manner dependent on the Paz2 modification system (Paz2-I). These and other results support the model that the identified membrane structure is necessary for sequestration of peroxisomes by the vacuolar membranes at stage 1c. Furthermore, we speculate that not only the Paz2 modification system but also other *APG*-homologous *PAZ* gene products are necessary at stage 1c to act through the membrane structure, because the corresponding *paz* mutants were blocked at stage 1c (Mukaiyama *et al*., 2002). The necessity of Apg gene products for microautophagy, a process in which no membrane formation (except vacuolar extension) has ever been identified, has not been well understood (Muller *et al*., 2000). Although Apg7 has been reported to be dispensable for some type of microautophagy (Roberts *et al*., 2003), the finding of membrane structure formed during micropexophagy and its relation to many Apg molecules rationalizes the convergence of these molecules with autophagosome formation in macroautophagy (Figure 9).

Several possibilities arose regarding the role of the membrane structure during micropexophagy at stage 1c. From our present results, we postulate that the membrane structure itself fuses with vacuolar membrane at the last stage of peroxisome sequestration, thus directly mediating vacuolar membrane fusion. Figure 9 represents one model of such membrane dynamics of vacuolar membrane and the membrane structure. This scheme was consistent with 1) the observed fluorescent dynamics of YFP-Paz2 and vacuolar membrane stained with FM4-64; 2) other fluorescent and EM images; and 3) the necessity of the membrane structure or Paz2 at stage 1c of micropexophagy. Other models in which the pexophagosome (not the membrane structure) fuses with vacuolar membrane during micropexophagy do not match with these results.

Otherwise, Paz2 might be more directly involved in homotypic fusion between opposing vacuolar membranes such as GATE16 (one of the mammalian orthologs of Paz2). In fact, GATE16 has been reported to act at the terminal phase of membrane fusion by forming a complex with two other fusion machinery components, NSF and GOS-28 (Muller *et al*., 2002). However, the precise details of these processes, and the precise involvement of the membrane structure in them, remain to be elucidated in the future.

Another finding in this study was the unique function of a ubiquitin-like protein, Paz2, that does not require the

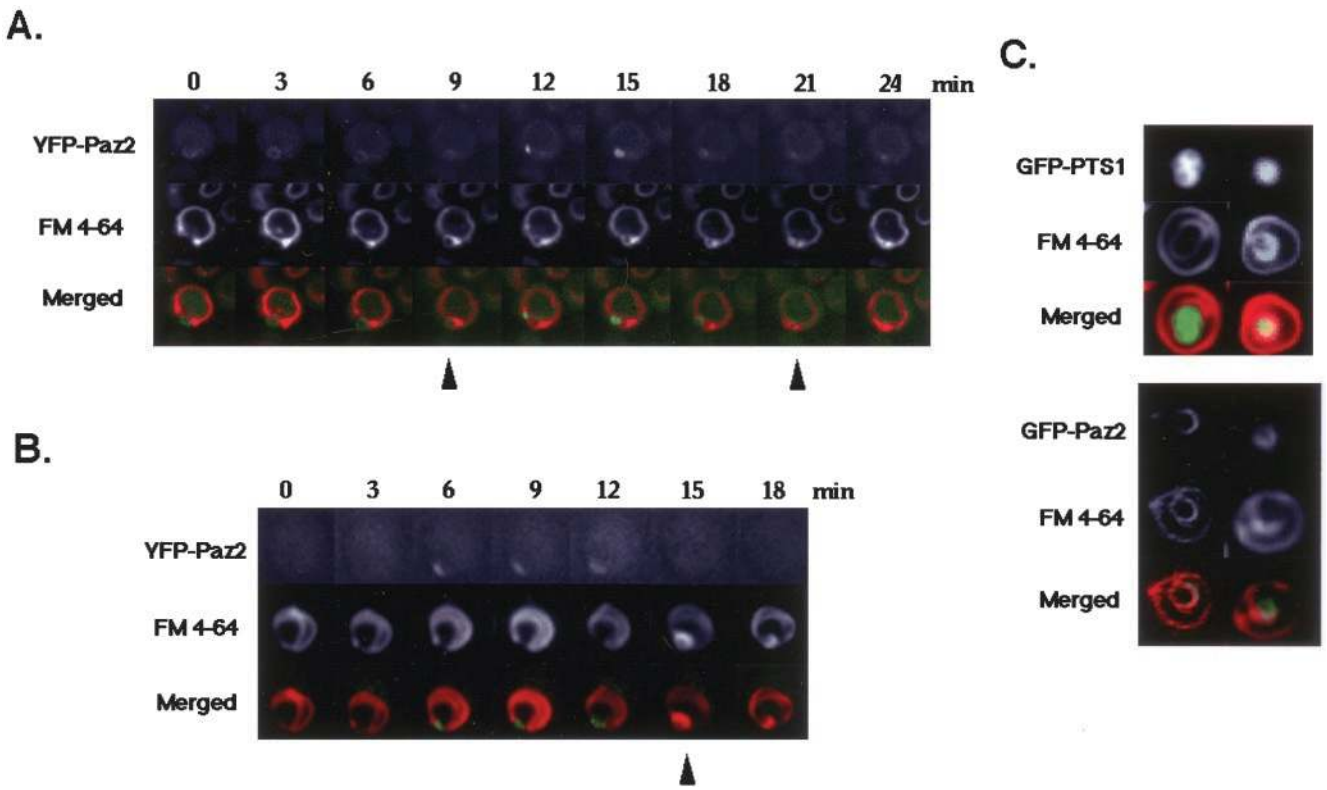

Figure 7. Single-cell observation of *P. pastoris* cells expressing YFP-Paz2 under the pexophagic conditions. Vacuolar membranes were prestained with FM 4–64. Cells of strain SA1017 were shifted to (A) ethanol-containing medium to induce macropexophagy or (B) glucose-containing medium to induce micropexophagy, incubated for ~30 min, and observed under fluorescent microscopy. YFP- and FM4-64-fluorescence are expressed as artificial green and red colors, respectively, in merged images. (A) Macropexophagy. An autophagosome (YFP-Paz2) was formed and fused with vacuolar membrane. At the time points indicated by arrow heads (9 and 21 min), FM4-64 fluorescence was distributed into autophagosome membrane forming a ring structure and YFP-Paz2 fluorescence diminished possibly due to diffusion into vacuolar membrane. Initiation of the second autophagosome formation was observed at 12 min. (B) Micropexophagy. At stage 1c indicated by arrow head (15 min), a cup-shaped structure was stained with FM4-64 and YFP-Paz2 fluorescence diminished suggesting fusion between the membrane structure and vacuolar membrane. (C) Top, a cup-shaped membrane structure attaching to a peroxisome was stained with FM4-64 in putative stage 2 cells. Bottom, a minor portion of cells at putative stage 2 (or stage 1c) gave a cup-shaped GFP-Paz2 fluorescence, which seemed to be incorporated into the vacuole.

Paz2 modification system. Depletion of Paz2 resulted in extensive vacuolar engulfment of peroxisomes and cytosol (Figure 8A). On the other hand, overexpression of Paz2 arrested vacuolar engulfment of peroxisomes at early stage 1 (Mukaiyama *et al*., 2002). GFP fluorescence was associated with the vacuolar membrane surface in GFP-Paz2 G116A-expressing cells (Figure 8C), and considerable amounts of Paz2-G116 and HA-Paz2 G116A were found in an LSP fraction containing vacuoles (Figure 2). Most importantly, Paz2 G116A, which did not receive the Paz2-modification to Paz2-I, restored normal vacuolar morphology in the *paz2*Δ cells (Figure 8B). From these genetical and morphological observations, we suggest a role for an unmodified form of Paz2 (Paz2 G116 or Paz2 G116A) as a negative regulator that suppresses vacuolar engulfment of peroxisomes during conditions that promote peroxisome proliferation (stage 0).

After a shift from glucose- to methanol-containing medium, macroautophagy occurs within 6 h, and the amount of Paz2-I as well as the total amount of Paz2 reaches a considerable level before the onset of micropexophagy. The intracellular level of Paz2 does not change after the onset of micropexophagy (Figure 1B). Therefore, switching of Paz2 function as negative regulator during stage 0 to its role as an essential factor for assembly of the membrane structure during late stage 1 is achieved through further activation of the Paz2 modification system and subsequent localization of Paz2 to the membrane structure. Indeed, the amount of HA-Paz2-I nearly doubled after the onset of micropexophagy (Figure 1B). These features are quite distinct from those of the Aut7-PE system in *S. cerevisiae*, in which macroautophagy is induced upon *AUT7* expression after nitrogen-starvation conditions.

What is the molecular basis for such spatiotemporal formation of the membrane structure? How is such a change in Paz2 localization regulated? The considerable overlap of *PAZ/GSA* genes with *APG/AUT/CVT* genes suggests that the process of membrane structure formation shares common mechanisms with that of autophagosome formation. Our biochemical and morphological studies are consistent with this, supporting a close functional relation of many *PAZ* gene products (at least Paz1 [Apg1], Paz2 [Aut7], Paz8 [Aut2], and Gsa7 [Apg7]) to the membrane structure. Recent studies have identified a preautophagosomal structure (PAS) essential for autophagosome membrane formation, which contains Aut7, Apg5, Apg12, Apg16, Apg1, Apg2, Apg9, Apg14, Cvt9,

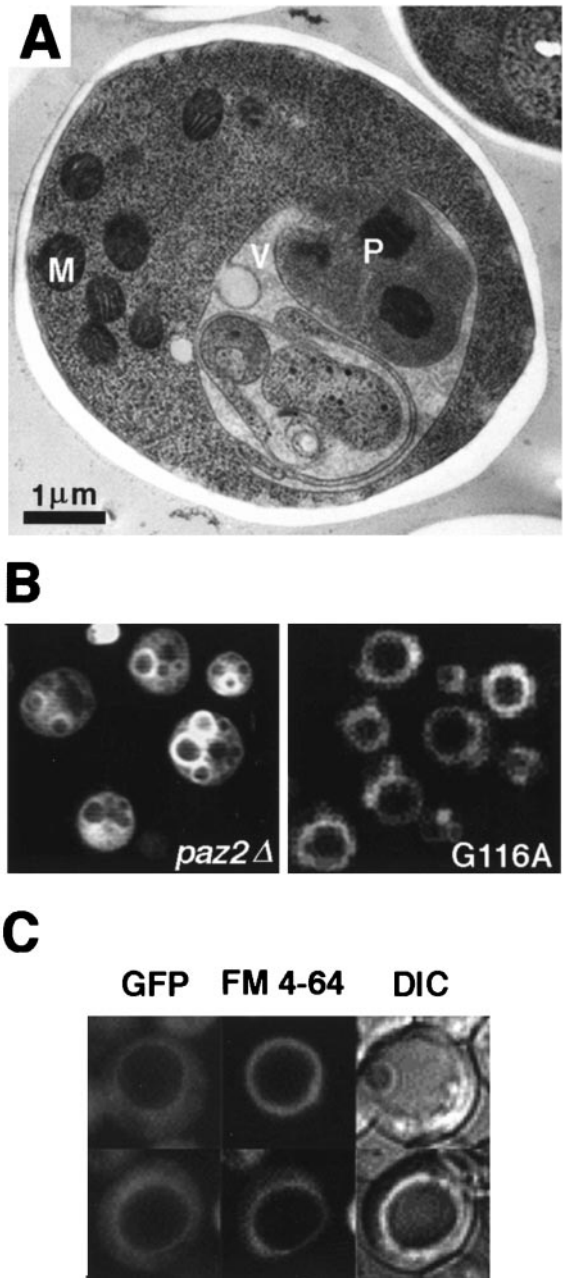

Figure 8. Aberrant vacuolar morphology of the *paz*2Δ cells was rescued by an uncleavable form of Paz2, GFP-Paz2 G116A. (A) EM image of the aberrant vacuolar morphology of *paz*2Δ cells (strain PPM5010) grown for 12 h on methanol-containing medium. P, peroxisome; V, vacuole; M, mitochondrion. (B) An uncleavable form of Paz2, GFP-Paz2 G116A, restored normal vacuolar morphology (strain PPM5017). Vacuolar membranes were stained with FM4-64. P, peroxisome; M, mitochondrion; V, vacuole. (C) Association of GFP fluorescence with the vacuolar membrane in GFP-Paz2 G116A cells (strain PPM5017).

and Cvt19, at least transiently, and have raised the possibility of de novo formation of membrane structures (Suzuki *et al*., 2001; Kim *et al*., 2002; Noda *et al*., 2002). In previous studies, we and others identified 10 PAS-containing proteins, among which six *Pichia* homologs were identified as *PAZ/GSA* genes (Table 1) (Stromhaug *et al*., 2001; Mukaiyama *et al*., 2002). By its definition, PAS undergoes "nucleation" and "assembly elongation" to become an autophagosome (Noda *et al*., 2002). In addition to the fact that the identified membrane structure attaches to peroxisomal membrane surface, the membrane structure that must be distinguished from PAS differs in its appearance both in size and shape. Autophagosomes have been observed as small fluorescent puncta when the appropriate Apg molecules are fluorescently labeled (Suzuki *et al*., 2001). The cup-shaped membrane structure is much larger than autophagosomes. Therefore, it is reasonable to postulate that the membrane structure is also formed from the PAS through "nucleation" and "assembly elongation" steps under spatio-temporal regulation distinct from the autophagosome formation.

Although the observed membrane structure and the isolation membrane formed during macropexphagy (or the pexophagosome membrane) seem to share common molecular components, there are notable differences between them. First, pexophagosome or autophagosome membranes sequester their cargos completely from the cytosol (Figures 3C and 7A). In contrast, the identified membrane structure was not observed to engulf peroxisomes completely in the micropexophagic process. Second, although the isolation membrane formed during macropexophagy cannot fuse with the vacuole until pexophagosome is formed, the membrane structure formed during micropexophagy fuses to the vacuole directly (Figures 7 and 9). These are critical characteristics of the membrane structure identified in this study that should distinct it from autophagosome and the isolation membrane formed during macroautophagy. Therefore, we suggest that the membrane structure is formed as a "micropexophagy-specific membrane apparatus" after induction of micropexophagy (Figure 9).

The identification of the Paz2 modification system (Paz2-I) and the micropexophagy-specific membrane apparatus has provided us a novel molecular and structural basis to study micropexophagy. Recently, we have shown that Paz4/Ugt51 is localized to the micropexophagy-specific membrane apparatus during micropexophagy (Oku *et al*., 2003). Further analyses of the regulation of the Paz2 modification system and membrane structure formation by other *PAZ* gene products, together with detailed structural analysis of the membrane structure, will give valuable insights into the common and specific mechanisms of both microautophagy and macroautophagy pathways.

ACKNOWLEDGMENTS

We thank Dr. T. Noda (National Institute for Basic Biology) for helpful discussion. We thank Dr. H. Yurimoto, M. Oku, Y. Ano, and other members of the Laboratory of Microbial Biotechnology (Kyoto University) for helpful advice and technical assistance. This research was supported in part by a Grant-in-Aid for Scientific Research (S) 13854008 and a Grant-in-Aid for Scientific Research on Priority Areas 12146202 to Y.S. from the Ministry of Education, Science, Sports and Culture of Japan, and the NIBB Cooperative Research Program, and by a "dynamic bio" project from the Ministry of Economy, Trade and Industry.

Note added in proof. After acceptance of this manuscript, yeast autophagy related genes have been unified as *ATG* (*aut*oph*a*g*y*-related) genes [D.J. Klionsky, *et al.* (2003). A unified nomenclature for yeast autophagy-related genes. Dev. Cell, 5, 539–545]. Accordingly, *PAZ2, PAZ8, GSA7/PAZ12,* and *GSA20* have been assigned as *PpATG8, PpATG4, PpATG7*, and *PpATG3*, respectively. Table 1 gives unified names for the other related genes.

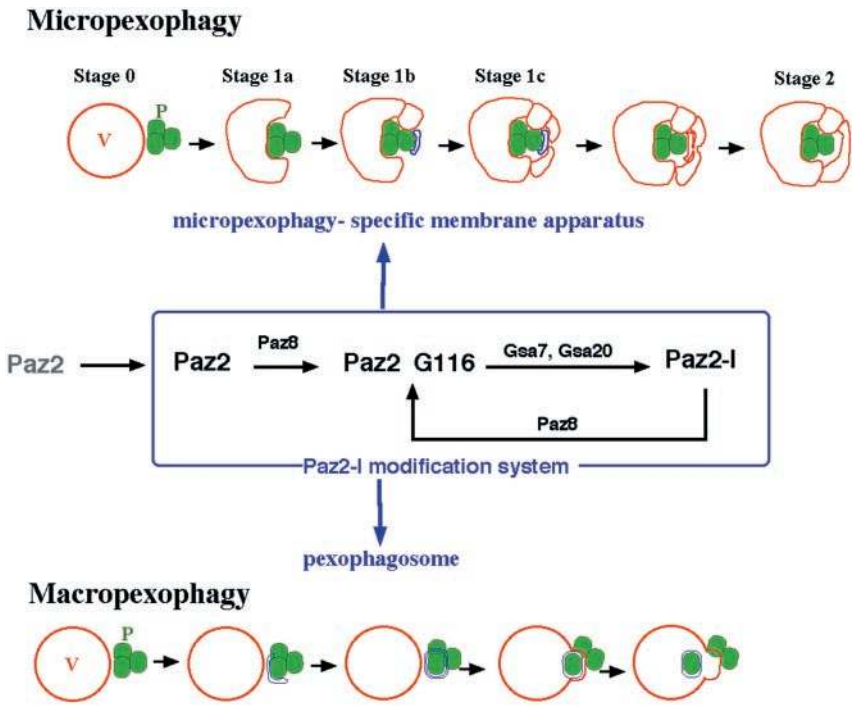

Figure 9. Role of the Paz2 modification system in micropexophagy and macropexophagy. After the onset of micropexophagy, Paz2 is recruited to the newly formed membrane structure upon Paz2 modification to Paz2-I and the concerted action of other *PAZ* gene products. The membrane structure formed as a micropexophagy-specific membrane apparatus is necessary for sequestration of peroxisomes from the cytosol. A possible sequestration scheme involving fusion events between the membrane structure and vacuole is presented. In macropexophagy: the Paz2 modification pathway (Paz2-I) is involved in pexophagosome formation. In both pexophagic processes, de novo membrane formation (represented as blue compartments) occurs under Paz2-modification system regulation. P, peroxisomes; V, vacuolar membrane.

REFERENCES

Baba, M., Osumi, M., Scott, S.V., Klionsky, D.J., and Ohsumi, Y. (1997). Two distinct pathways for targeting proteins from the cytoplasm to the vacuole/lysosome. J. Cell Biol. *139*, 1687–1695.

George, M.D., Baba, M., Scott, S.V., Mizushima, N., Garrison, B.S., Ohsumi, Y., and Klionsky, D.J. (2000). Apg5p functions in the sequestration step in the cytoplasm-to-vacuole targeting and macroautophagy pathways. Mol. Biol. Cell *11*, 969–982.

Gould, S.J., McCollum, D., Spon, A.P., Heyman, J.A., and Subramani, S. (1992). Development of the yeast *Pichia pastoris* as a model organism for a genetic and molecular analysis of peroxisome assembly. Yeast *8*, 613–628.

Horazdovsky, B.F., and Emr, S.D. (1993). The VPS16 gene product associates with a sedimentable protein complex and is essential for vacuolar protein sorting in yeast. J. Biol. Chem. *268*, 4953–4962.

Huang, W.-P., Scott, S.V., Kim, J., and Klionsky, D.J. (2000). The itinerary of a vesicle component, Aut7p/Cvt5p, terminates in the yeast vacuole via the autophagy/Cvt pathways. J. Biol. Chem. *275*, 5845–5851.

Ichimura, Y., *et al*. (2000). A ubiquitin-like system mediates protein lipidation. Nature *408*, 488–492.

Kim, J., Huang, W.P., Stromhaug, P.E., and Klionsky, D.J. (2002). Convergence of multiple autophagy and cytoplasm to vacuole targeting components to a perivacuolar membrane compartment prior to de novo vesicle formation. J. Biol. Chem. *277*, 763–773.

Kim, J., Kamada, Y., Stromhaug, P.E., Guan, J., Hefner-Gravink, A., Baba, M., Scott, S.V., Ohsumi, Y., Dunn, W.A., Jr., and Klionsky, D.J. (2001). Cvt9/gsa9 functions in sequestering selective cytosolic cargo destined for the vacuole. J. Cell Biol. *153*, 381–396.

Kirisako, T., Baba, M., Ishihara, N., Miyazawa, K., Ohsumi, M., Yoshimori, T., Noda, T., and Ohsumi, Y. (1999). Formation process of autophagosome is traced with Apg8p/Aut7p in yeast. J. Cell Biol. *147*, 435–446.

Kirisako, T., Ichimura, Y., Okada, H., Kabeya, Y., Mizushima, N., Yoshimori, T., Ohsumi, M., Takao, T., Noda, T., and Ohsumi, Y. (2000). The reversible modification regulates the membrane-binding stage of Apg8/Aut7 essential for autophagy and the cytoplasm to vacuole targeting pathway. J. Cell Biol. *151*, 263–275.

Klionsky, D.J., and Ohsumi, Y. (1999). Vacuolar import of proteins and organelles from the cytoplasm. Annu. Rev. Cell Dev. Biol. *15*, 1–32.

Mortimore, G.E., Hutson, N.J., and Surmacz, C.A. (1983). Quantitative correlation between macro- and microautophagy in mouse hepatocytes during starvation and refeeding. Proc. Natl. Acad. Sci. USA *80*, 2179–2183.

Mortimore, G.E., Lardeux, B.R., and Adams, C.E. (1988). Regulation of microautophagy and basal protein turnover in rat liver: effects of short-term starvation. J. Biol. Chem. *263*, 2506–2512.

Mukaiyama, H., Oku, M., Samizo, T., Hammond, A.T., Glick, B.S., Kato, N., and Sakai, Y. (2002). Paz2 and 13 other PAZ gene products regulate vacuolar engulfment of peroxisomes during micropexophagy. Genes Cells *7*, 75–90.

Muller, J.M., Shorter, J., Newman, R., Deinhardt, K., Sagiv, Y., Elazar, Z., Warren, G., and Shima, D.T. (2002). Sequential SNARE disassembly and GATE-16-GOS-28 complex assembly mediated by distinct NSF activities drives Golgi membrane fusion. J. Cell Biol. *157*, 1161–1173.

Muller, O., Satler, T., Flotenmeyer, M., Schwarz, H., Plattner, H., and Mayer, A. (2000). Autophagic tubes: vacuolar invaginations involved in lateral membrane sorting and inverse vesicle budding. J. Cell Biol. *151*, 519–528.

Noda, T., Suzuki, K., and Ohsumi, Y. (2002). Yeast autophagosomes: *de novo* formation of a membrane structure. Trends Cell Biol. *12*, 231–235.

Ohsumi, Y. (2001). Molecular dissection of autophagy: two ubiquitin-like systems. Nat. Rev. Mol. Cell Biol. *2*, 211–216.

Oku, M., Warnecke, D., Noda, T., Müller, F., Heinz, E., Hiroyuki Mukaiyama, Kato, N., and Sakai, Y. (2003). Peroxisome degradation requires catalytically active sterol glucosyltransferase with a GRAM domain. EMBO J. *22*, 3231–3241.

Roberts, P., Moshitch-Moshkovitz, S., Kvam, E., O'Toole, E., Winey, M., and Goldfarb, D.S. (2003). Piecemeal microautophagy of nucleus in *Saccharomyces cerevisiae*. Mol. Biol. Cell *14*, 129–141.

Sakai, Y., Kazarimoto, T., and Tani, Y. (1991). Transformation system for an asporogenous methylotrophic yeast, *Candida boidinii*: cloning of the orotidine-5'-phosphate decarboxylase gene (URA3), isolation of uracil auxotrophic mutants, and use of the mutants for integrative transformation. J. Bacteriol. *173*, 7458–7463.

Sakai, Y., Koller, A., Rangell, L.K., Keller, G.A., and Subramani, S. (1998). Peroxisome degradation by microautophagy in *Pichia pastoris*: identification of specific steps and morphological intermediates. J. Cell Biol. *141*, 625–636.

Sakai, Y., and Subramani, S. (2000). Environmental response of yeast peroxisomes: aspects of organelle assembly and degradation. Cell Biochem. Biophys. *32*, 51–61.

Stromhaug, P.E., Bevan, A., and Dunn, W.A., Jr. (2001). GSA11 encodes a unique 208-kDa protein required for pexophagy and autophagy in *Pichia pastoris*. J. Biol. Chem. *276*, 42422–42435.

Subramani, S. (1998). Components involved in peroxisome import, biogenesis, proliferation, turnover, and movement. Physiol. Rev. *78*, 171–188.

Suzuki, K., Kirisako, T., Kamada, Y., Mizushima, N., Noda, T., and Ohsumi, Y. (2001). The pre-autophagosomal structure organized by concerted functions of *APG* genes is essential for autophagosome formation. EMBO J. *20*, 5971–5981.

Toyooka, K., Okamoto, T., and Minamikawa, T. (2001). Cotyledon cells of *Vigna mungo* seedlings use at least two distinct autophagic machineries for degradation of starch granules and cellular components. J. Cell Biol. *154*, 973–982.

Tuttle, D.L., and Dunn, W.A. (1995). Divergent modes of autophagy in the methylotrophic yeast *Pichia pastoris*. J. Cell Sci. *108*, 25–35.

Yuan, W., Stromhaug, P.E., and Dunn, W.A.J. (1999). Glucose-induced autophagy of peroxisomes in *Pichia pastoris* requires a unique E1-like protein. Mol. Biol. Cell *10*, 1353–1366.